

# Novel phytochemical *Cissus quadrangularis* extract–loaded chitosan/Na-carboxymethyl cellulose–based scaffolds for bone regeneration

Sedef Tamburaci<sup>1,2</sup>, Ceren Kimna<sup>2</sup>  
and Funda Tihminlioglu<sup>2</sup>

Journal of Bioactive and  
Compatible Polymers  
2018, Vol. 33(6) 629–646  
© The Author(s) 2018  
Article reuse guidelines:  
sagepub.com/journals-permissions  
DOI: 10.1177/0883911518793913  
journals.sagepub.com/home/jbc



## Abstract

Medicinal plants are attracting considerable interest as a potential therapeutic agent for bone tissue regeneration. *Cissus quadrangularis* L. is also a medicinal plant known with its osteogenic activity. In this study, a phytochemical scaffold was produced by incorporating *Cissus quadrangularis* with chitosan/Na-carboxymethyl cellulose blend by lyophilization technique. The effect of *Cissus quadrangularis* loading on the mechanical, morphological, chemical, and degradation properties as well as in vitro cytotoxicity, cell proliferation, and differentiation of the composites was investigated. Scanning electron microscopy images showed that porous *Cissus quadrangularis*–loaded scaffolds were obtained with an average pore size of 148–209  $\mu\text{m}$  which is appropriate for bone regeneration. *Cissus quadrangularis* incorporation enhanced the compression modulus of scaffolds from 76 to 654 kPa. In vitro cell culture results indicated that *Cissus quadrangularis*/chitosan/Na-carboxymethyl cellulose scaffolds provided a favorable substrate for the osteoblast adhesion, proliferation, and mineralization. Results supported the osteoinductive property of the *Cissus quadrangularis* extract–incorporated scaffolds even without osteogenic media supplement. *Cissus quadrangularis* extract increased the alkaline phosphatase activity of the SaOS-2 cells on scaffolds on 7th and 14th days of incubation. The investigation of characterization and cell culture studies suggest that *Cissus quadrangularis*–loaded osteoinductive *Cissus quadrangularis*/chitosan/Na-carboxymethyl cellulose scaffold can serve as a potential biomaterial for bone tissue engineering applications.

<sup>1</sup>Biotechnology and Bioengineering Graduate Program, İzmir Institute of Technology, İzmir, Turkey

<sup>2</sup>Department of Chemical Engineering, İzmir Institute of Technology, İzmir, Turkey

## Corresponding author:

Funda Tihminlioglu, Department of Chemical Engineering, İzmir Institute of Technology, Gülbahçe Campus, Urla 35430, İzmir, Turkey.

Email: fundatihminlioglu@iyte.edu.tr

## Keywords

*Cissus quadrangularis*, scaffold, bone, chitosan, Na-carboxymethyl cellulose

## Introduction

Recently, bone tissue engineering has focused on the evaluation of the natural polymer-based bioactive composite scaffolds to provide an osteogenic effect at the defect site. Among natural polymers, chitosan (CHI) and carboxymethyl cellulose are the remarkable polymers in terms of their structural similarity to the extracellular matrix, leading to biocompatibility. CHI is a natural polymer, with a linear structure consisting of  $\beta(1-4)$  glycosidic bonds linked to D-glucosamine residues with a variable number of randomly located N-acetyl-D-glucosamine (NAG) groups.<sup>1</sup> It is reported that CHI-based scaffolds are appropriate for cell adhesion, proliferation, and mineralization with its bioactive, biodegradable, anti-bacterial, biocompatible properties, and a hydrophilic surface which is absent in many synthetic polymers.<sup>2-5</sup> Na-carboxymethyl cellulose (Na-CMC), obtained by the chemical modification of the natural cellulose, is a natural biodegradable and biocompatible anionic polymer and the only water-soluble derivative of cellulose.<sup>6</sup> Since it has a very similar structure with CHI, it strongly reacts and acts as an ionic crosslinking agent at the appropriate pH.<sup>7-9</sup> This polyelectrolyte complex formation occurs with the ionic cross-linking between CHI and Na-CMC that increases the stability. Na-CMC and CHI blends in bone tissue engineering applications are preferred for their strong interactions.<sup>10</sup>

Generally, stimulating agents are needed to increase the osteogenic activity of the bone tissue formation. The utilization of the phytochemical extracts as osteogenic agents became widely important. *Cissus quadrangularis* L. (CQ) is a medicinal plant from *Vitaceae* family and has been used as a medicinal plant for centuries in India and Africa.<sup>11,12</sup> It is used for bone fracture healing and joint health, osteoporosis prevention, antimicrobial, analgesic, anti-inflammatory, antioxidant, and the tissue protective in traditional medicine. Generally, alcoholic (ethanol, methanol) extracts of CQ are widely used in the commercial market for these applications.<sup>13-18</sup> CQ includes vitamins and steroids, which are found to have a specific effect on bone fracture healing. Fracture healing studies suggest that its unidentified anabolic steroids may act on estrogenic receptors of the bone.<sup>19</sup> The photochemical analysis of plant has indicated that CQ includes high amounts of ascorbic acid, carotene, anabolic steroidal substances, vitamin C, potassium, calcium, zinc, sodium, iron, lead, cadmium, copper, calcium oxalate, and magnesium.<sup>20</sup> The stem extract of CQ contains a high percentage of calcium ions (ca. 4% by weight) and phosphorus ions, and they are both essential for bone fracture healing.<sup>21</sup> In addition, it was reported that CQ stem includes two asymmetric tetracyclic triterpenoids and two steroidal principles.<sup>22</sup> The active constituents of CQ extract still remain unclear, and it is thought that several compounds of CQ show the synergistic effect. The quantification of the major phytosterols,  $\beta$ -sitosterol, and stigmasterol is important for the bone fracture treatment as they can bind to osteoblasts and stimulate the growth and the proliferation since they are precursors of anabolic steroidal substances.<sup>23-25</sup> In a study, regulatory effects of CQ on insulin-like growth factor (IGF) system components in osteoblasts which are important factors for bone development and remodeling were investigated and the increase in IGF expression could be attributed to phytoestrogens of the plant.<sup>26</sup> Efficacy of CQ administration by intramuscular injection on early ossification and bone remodeling in vivo studies indicated that CQ acts on stimulation of metabolism and increases the uptake of calcium, sulfur, and strontium by the osteoblasts in fracture healing.<sup>27,28</sup> Besides, CQ extract enhanced the bone marrow mesenchymal stem cell proliferation and fetal bone growth.<sup>29</sup> In vivo studies showed the CQ extract has influence in fracture healing

rate, antiosteoporotic effects on bone, and periodontal regeneration.<sup>28–34</sup> In the literature, there are a limited number of studies related to CQ incorporation to polymer scaffolds. Only polycaprolactone (PCL) and alginate/*O*-carboxymethyl CHI blend scaffolds have been reported for bone tissue engineering applications.<sup>35,36</sup>

In this study, it is proposed to fabricate a porous, bioactive CQ extract–loaded CHI/Na-CMC blend scaffolds for bone tissue engineering applications. CHI and Na-CMC polymers were used to form polyelectrolyte complex in order to overcome the stability problem without a crosslinking agent. The aim of the study is to evaluate the osteogenic effect of CQ extract incorporation as an alternative bioactive agent on cell growth, proliferation, and mineralization as well as on the morphological, physical, chemical, and mechanical properties of fabricated CQ-loaded CHI/Na-CMC scaffolds.

## Materials and methods

### Materials

Commercial low molecular weight (LMW) CHI powder (50,000–190,000 Da) with deacetylation degree of 75%–85% and Na-CMC (Sigma-Aldrich), CQ extract (3% ketosteroid content; Ambe Phytoextracts Pvt.), and acetic acid (analytical grade; Sigma-Aldrich) used for the preparation of scaffolds. Lysozyme (Sigma-Aldrich; from chicken egg white), sodium azide (Sigma-Aldrich), and phosphate-buffered solution (10×) (PBS tablets; Invitrogen, Thermofisher Scientific) were used for biodegradation studies. PBS solution (Sigma-Aldrich) was used for swelling studies. SaOS-2 cell line (ATCC® HTB-85™) with cell culture supplements; Dulbecco's modified Eagle's medium (DMEM, Sigma-Aldrich) and minimum essential medium (MEM; Sigma-Aldrich), fetal bovine serum (FBS, Lonza), penicillin–streptomycin solution (Lonza), and L-glutamine (Lonza) were used for cell culture studies. WST-1 cell proliferation reagent (BioVision Inc.), Resazurin Cell Viability Kit (Cell Signaling Technology Inc.), and ALP-Enzyline PAL optimize kit (Biomerieux Inc.) were used for in vitro assays. Silver nitrate (Sigma-Aldrich), sodium thiosulfate (Sigma-Aldrich), and Alizarin Red S (Sigma-Aldrich) were used for staining protocols.

### Preparation of CQ/CHI/Na-CMC scaffold

First, 2 g LMW CHI was dissolved in 48 mL of deionized water and mixed with the 50 mL of 2% (w/v) of Na-CMC aqueous solution. Second, 2 mL of acetic acid was added to the mixture dropwise and stirred for 15 min to dissolve CHI in blend,<sup>10</sup> and 0.5% and 1% (w/v) of CQ extract were carefully added to the CHI/Na-CMC blend with continual stirring. The solution was mixed for 30 min and filled in well plates then frozen at –20°C for 24 h. The frozen scaffolds were lyophilized in a freeze dryer (Labconco Inc.) for 48 h. The scaffolds were stored in a desiccator for further characterization tests.

### Characterization

**Scanning electron microscopy analysis.** The surface morphology and biomineralization of the scaffolds were investigated by scanning electron microscopy (SEM; Quanta FEG). The scaffolds were cut horizontally with a thickness of 3 mm, and then coated with a thin layer of gold with a current of 15 mA under vacuum. The pore size distributions of the scaffolds were measured using the scanning electron micrographs by Image J software.

**Fourier transform infrared spectroscopy and gas chromatography analyses.** The chemical structure of the samples was analyzed by a Fourier transform infrared spectroscopy (FT-IR) using ATR attachment (Shimadzu FTIR-8400S) at wavelengths ranging from 4000 to 650  $\text{cm}^{-1}$  at a resolution of 4  $\text{cm}^{-1}$  with 20 scans.

Gas chromatography–mass spectrometry (GC-MS) analysis of ethanolic extract was carried out with GC-MS (Agilent 6890N/5973N Network) with a GC column HP-5MS (5% phenyl 95% methyl polysiloxane) and Agilent 5973 Mass Selective Detector (S/SL inlet) was used. The other conditions were as follows: oven temperature 110°C–270°C at the ratio of 10°C/min; injector temperature 250°C; carrier gas flow Helium at 1 mL/min; Mass Scan 25–450; MS Time 50 min. The spectrum of the desired components was compared with the NIST library database.

**Compression test.** The mechanical strength of scaffolds was measured according to the ASTM-D 5024-95a standard. TA XT Plus Texture Analyzer (Stable Micro Systems) was used for a compression test with 1/2" cylindrical delrin probe. Mechanical compression data are described as an average of five test specimens with standard error. Tests were performed with a cross-head speed of 5 mm/min at room temperature and compressed up to 75% of original height. Dry samples and hydrated samples (immersed in PBS, pH 7.4) were tested. Scaffolds were hydrated in PBS solution (pH 7.4, at 37°C) for 1 h prior to testing and kept immersed in PBS throughout the test. Compressive stress–strain curves were plotted and compressive elastic modulus ( $E^*$ ) was determined for all scaffolds.

**Water uptake capacity and enzymatic degradation.** Swelling studies were carried out in PBS solution (pH 7.4) at 37°C. Previously, scaffolds were stabilized with 100% ethanol, dried, and weighed. Then, they were soaked into PBS and preserved in an incubator at 37°C. Wet scaffolds were weighed for 24 and 48 h. The water uptake capacity % ( $W_{\text{up}}$ ) of the scaffolds was calculated for each time point using following equation

$$W_{\text{up}} = \left[ \frac{(\text{wet weight} - \text{dry weight})}{(\text{dry weight})} \right] \times 100 \quad (1)$$

In order to observe the enzymatic degradation, the weight changes of the scaffolds were measured at specific time intervals. Scaffolds were weighed and put into PBS solution with 1.5 mg/L lysozyme. Sodium azide of 0.1% (w/v) was added to prevent the bacterial contamination. Samples were put in a shaking incubator at 37°C and weighed for a time period of 7, 14, and 21 days. The weight loss % in degradation process was calculated according to the equation below

$$\text{Weight loss \%} = \frac{\text{initial weight} - \text{dry weight}}{\text{initial weight}} \times 100 \quad (2)$$

### ***In vitro studies***

The scaffolds were sterilized with ethylene oxide before used. SaOS-2 cell line was used as osteoblast model for in vitro studies.

***In vitro cytotoxicity determination.*** Cytotoxicity of scaffolds on SaOS-2 cells was evaluated by indirect extraction method (ISO 10993; 24 h extraction of scaffolds in cell culture medium) with the WST 1 assay that is based on the conversion of stable tetrazolium to a soluble formazan by a

complex cellular mechanism that occurs primarily at the cell surface and this bioreduction is largely dependent on the glycolytic production of NAD(P)H in viable cells.<sup>37</sup> Cell seeding was carried out at  $10^5$  cell/mL cell density and incubated on 96-well plates with 100  $\mu$ L extraction medium for 72 h. Optical density determined at 440 nm was normalized to cell viability % from the following equation

$$CV \% = \frac{(\text{ABS of treated cells})}{(\text{ABS of control cells})} \times 100 \quad (3)$$

where the CV is cell viability and ABS is average absorbance value.

**Cell attachment, spreading, and proliferation on scaffolds.** Cell attachment and spreading on scaffolds were determined by fluorescence microscopy. SaOS-2 cells were seeded on scaffolds at a density of  $2.5 \times 10^6$  cell/mL and incubated for attachment for 4 h. Then, scaffolds were incubated in 500  $\mu$ L of cell culture medium for 7 days. The SaOS-2 cells on scaffolds were fixed with 3.7% paraformaldehyde (w/v in PBS) for 20 min at room temperature before staining. Cells incubated on scaffolds for 7 days were stained with DAPI (4',6-diamidino-2-phenylindole) fluorescence stains to detect nuclei.

Cell proliferation on scaffolds for 7, 14, 21, and 28 days of incubation was determined by using Resazurin Cell Viability Kit (Cell Signaling Technology Inc.). The blue non-fluorescent resazurin reagent is reduced to highly fluorescent resorufin by dehydrogenase enzymes in metabolically active cells. This conversion occurs in viable cells and the amount of resorufin produced is proportional to the number of viable cells in the sample. The resorufin formed in the assay was quantified by measuring the relative fluorescence units (RFU) using a fluorescence plate reader (Varioskan Flash) at 530–570 nm excitation and 590–620 nm emission.

**Alkaline phosphatase activity.** The differentiation of SaOS-2 cells was evaluated by measuring ALP activity by ALP-Enzyline PAL optimize kit (Biomérieux Inc.) at 7-, 14-, 21-, and 28-day incubation periods. ALP activity detection is based on hydrolysis of *p*-nitrophenyl phosphate (pNPP) to *p*-nitrophenol, the conversion of *p*-nitrophenol is directly proportional to ALP activity. The SaOS-2 cells were seeded at a density of  $2.5 \times 10^6$  cell/mL, incubated in the absence of osteogenic agents and the absorbance of the medium was measured by a plate reader (Varioskan Flash) at 405 nm.

**In vitro mineralization with von Kossa and Alizarin red staining.** von Kossa staining was used to detect calcification amount by cells by the silver nitrate reaction with phosphate deposition which is generally used for determination of “calcification” and bone-like mineral formation by cells. However, this deposition does not necessarily imply the presence of calcium or hydroxyapatite.<sup>38,39</sup> Therefore, Alizarin red staining method is used to verify the calcium deposition together with von Kossa staining for 14th day of incubation qualitatively. Before staining procedure, scaffolds were washed with  $1 \times$  PBS solution and fixed with 3.7% paraformaldehyde for 20 min at room temperature. In von Kossa staining procedure, scaffolds were incubated with 1% (w/v) aqueous silver nitrate solution for 30 min under ultraviolet (UV) light in laminar flow cabinet. Then, scaffolds were rinsed with distilled water and incubated with 5% (w/v) sodium thiosulfate solution for 5 min at room temperature to remove unreacted silver. In alizarin red S staining procedure, scaffolds were stained with 2% (w/v) aqueous alizarin red S solution by incubating at room temperature in the dark for 30 min. Finally, scaffolds were washed with distilled water and observed under stereomicroscope (SOIF DA 0737) for detecting a yellow-brownish and red stain detection, respectively. Energy dispersive X-ray fluorescence (ED-XRF) analysis was performed for 7th and 14th days in order to detect the calcium content % quantitatively.

### Statistical analysis

All experiments were repeated thrice and samples were evaluated in triplicate. The experimental data are expressed as the standard error of the mean (SEM). Statistical analyses of *in vitro* studies were carried out using two-way analysis of variance (ANOVA) with Tukey's multiple comparison tests ( $p < 0.05$ ).

## Results and discussion

### Morphology and pore size distribution

Scaffold morphology was analyzed using the SEM. Figure 1 shows the SEM images of unloaded and CQ-loaded CHI/Na-CMC scaffolds with two different CQ weight percentages. Scaffold slices cut from the cross-sectional area of the middle region were analyzed and it was observed that the scaffolds were obtained with porous and interconnected architecture. Average pore size distribution of scaffolds was determined by Image J using SEM images and depicted in Table 1. Porous scaffolds with an average pore size range of 148–209  $\mu\text{m}$  were obtained by CQ extract incorporation. It was reported that the optimum pore size should be in the range of 75–250  $\mu\text{m}$  for optimum bone growth.<sup>40</sup> In this study, the pore size of the scaffolds is in the range of 148–237  $\mu\text{m}$ , and therefore, it was found to be proper for bone tissue regeneration.

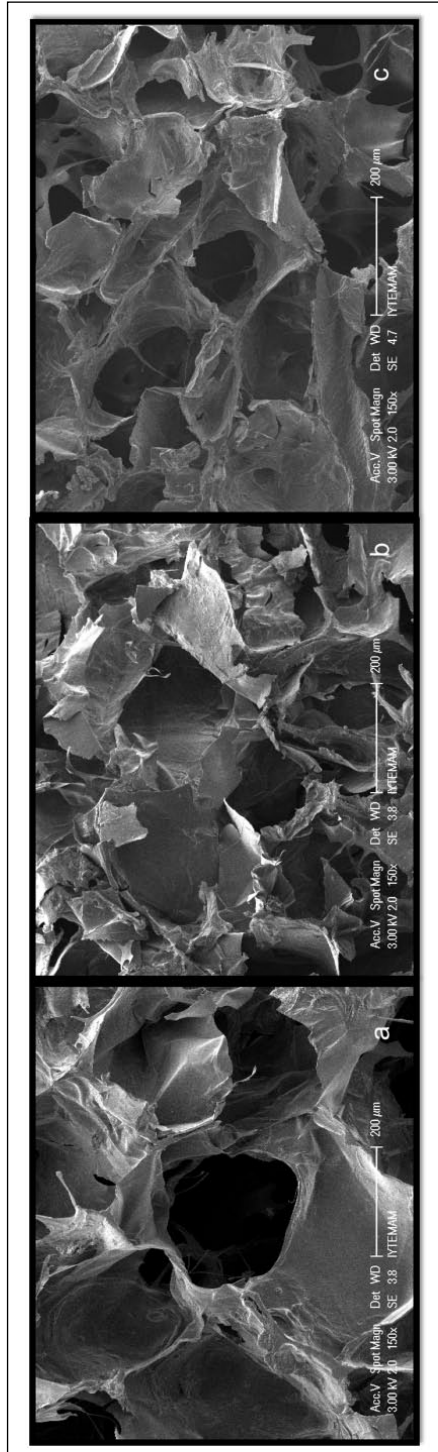
### Chemical characterization with FT-IR and GC analyses

The FT-IR spectra of CHI, Na-CMC, and CHI/Na-CMC scaffolds are shown in Figure 2. The attraction between  $-\text{NH}_3$  group of CHI and  $-\text{COO}-$  group of Na-CMC resulted with the polyelectrolyte complex formation was depicted with the IR bands of CHI, Na-CMC, and CHI/Na-CMC. The characteristic bands of CHI and Na-CMC were observed in the spectra of CHI/Na-CMC blend. The main bands appearing in the spectrum of CHI powder is due to N–H bending in amine groups at  $1560\text{ cm}^{-1}$ , C–O stretch of acetyl group in amide II bonds at  $1641\text{ cm}^{-1}$ , and C=O stretching in amide I bond at  $1655\text{ cm}^{-1}$ , respectively. The characteristic peak of Na-CMC due to  $\text{COO}^-$  symmetric stretching was observed at  $1415\text{ cm}^{-1}$ . The band at  $1588\text{ cm}^{-1}$  at the spectra of CHI/Na-CMC indicated that the intermacromolecular complex was occurred due to electrostatic interactions between the groups of cationic CHI and anionic Na-CMC. Thus, the stability of the polyelectrolyte complex is assured with the hydrogen bonding.<sup>41</sup>

The active components of the plant were identified qualitatively by GC-MS and compounds may supposed to be responsible for the activities were detected. It was found that the GC-MS chromatogram of the ethanolic extract of CQ had approximately 161 peaks. The major compounds were found as phytol, stigmaterol,  $\beta$ -sitosterol, and  $\alpha$ -amyrin and are listed in Table 2 with their retention time, percent peak area, molecular weight, and molecular formula. It was seen that  $\beta$ -sitosterol is the major steroidal compound in the CQ extract. Our findings agree with the phytochemical investigations of the extract revealing the presence of phytol,<sup>42</sup> stigmaterol,<sup>43</sup>  $\beta$ -sitosterol, and  $\alpha$ -amyrin.<sup>15</sup>  $\beta$ -sitosterol has been found to be principal ketosteroid in CQ.<sup>18,44</sup> It is thought that the anabolic steroidal compounds enhance the fracture healing by influence early regeneration and quicker mineralization of bone callus.<sup>45</sup>

### Mechanical properties

The effect of CQ extract on mechanical properties of scaffolds was determined by compression test. Compression modulus data showed that increasing CQ extract loading significantly enhanced

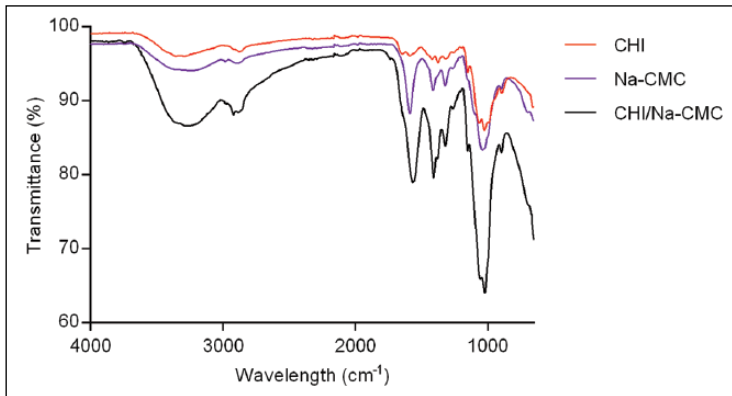


**Figure 1.** Scanning electron micrographs of (a) CHI/Na-CMC, (b) 0.5% CQ, and (c) 1% CQ extract-loaded CHI/Na-CMC scaffolds, respectively.

**Table 1.** Average pore size distribution of CHI/Na-CMC, 0.5% and 1% CQ extract-loaded CHI/Na-CMC scaffolds.

Groups	Average pore size ( $\mu\text{m}$ )
CHI/Na-CMC control	$237 \pm 57$
CHI/Na-CMC 0.5% CQ	$209 \pm 49$
CHI/Na-CMC 1% CQ	$148 \pm 32$

CHI/Na-CMC: chitosan/Na-carboxymethyl cellulose; CQ: *Cissus quadrangularis*.

**Figure 2.** FT-IR spectra of CHI, Na-carboxymethyl cellulose, and interaction of CHI and Na-CMC.**Table 2.** GC peaks of main components of *Cissus quadrangularis* extract.

S. no.	Name	RT (min)	MW (g/mol)	Molecular formula	Peak area (%)
1	Phytol	21.02	296.539	$\text{C}_{20}\text{H}_{40}\text{O}$	0.48
2	Stigmasterol	40.31	412.702	$\text{C}_{29}\text{H}_{48}$	0.73
3	$\beta$ -sitosterol	41.53	414.718	$\text{C}_{29}\text{H}_{50}$	4.03
4	$\alpha$ -amyrin	43.17	426.729	$\text{C}_{30}\text{H}_{50}$	1.20

GC: gas chromatography; MW: molecular weight, RT: residence time.

the mechanical strength of CHI/Na-CMC scaffolds for both wet and dry conditions. Compression moduli of dry CHI/Na-CMC scaffolds increased eightfold by 1% CQ extract loading from 76.5 to 654.4 kPa (Figure 3(a)). This increase in compression moduli of wet scaffolds was found nearly 3.5-fold by 1% CQ loading from 25 to 87.65 kPa when compared to CHI/Na-CMC control group (Figure 3(b)). This mechanical effect can be attributed to the microstructural alterations which increased the surface area of pore walls and decreased the pore size. Similarly, Suganya et al.<sup>35</sup> investigated tensile stress and Young moduli of CQ extract-loaded nanofibrous PCL scaffolds and indicated that CQ extract loading enhanced the tensile stress from 0.79 to 2.92 MPa and Young's modulus from 11.61 to 12.66 MPa.

### Water uptake capacity and enzymatic degradation

Swelling test with PBS solution was carried out to determine the water uptake capacity ( $W_{\text{up}}$ ) % of the CQ-loaded scaffolds by calculating the weight change. Figure 4 shows the water uptake



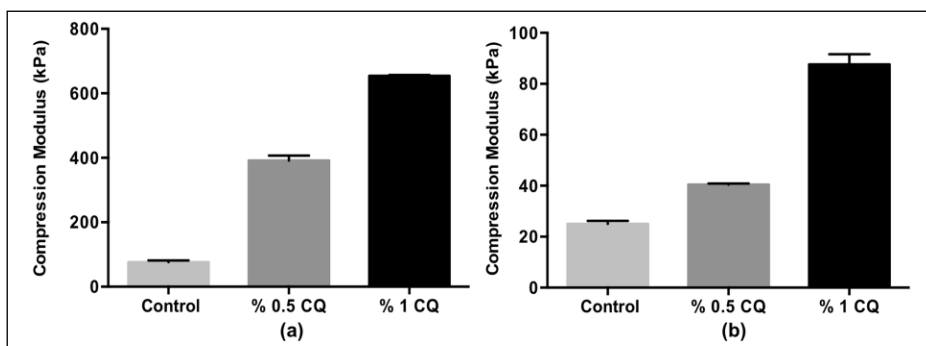


**Figure 3.** Compression moduli of CHI/Na-CMC, 0.5% and 1% CQ-loaded CHI/Na-CMC scaffolds in dry (a) and wet (b) condition.

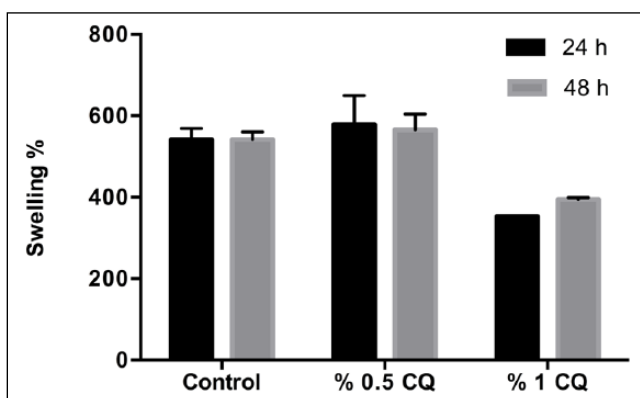


**Figure 4.** Swelling % of CHI/Na-CMC, 0.5% and 1% CQ-loaded CHI/Na-CMC scaffolds for 24- and 48-h incubation periods.

capacity % of scaffolds for 24- and 48-h incubation periods. Water uptake capacity is an important factor for the interaction of scaffold and surrounding tissue fluids. Results showed that water uptake capacity of scaffolds is almost same for 24- and 48-h incubation periods. Similar findings were obtained with the CQ extract addition in alginate/*O*-carboxymethyl CHI scaffolds.<sup>36</sup> Water uptake capacity % of control and 0.5% CQ-loaded groups were found as 541.6 and 565.8, respectively. Whereas the 1% CQ-loaded groups showed lower swelling % as 394.2 at 48 h of incubation. This can be attributed to the rigidity and microstructural alterations obtained in 1% CQ scaffold.

Enzymatic degradation study was carried out to determine the degradation behavior of CQ-loaded CHI/Na-CMC scaffolds for 21 days with degradation medium-containing lysozyme. Scaffolds showed similar weight loss % for the 7th day of degradation. However, CQ extract loading increased the weight loss for 14 and 21 days of degradation periods due to the possible dissolution of extract (Figure 5). The scaffolds also showed structural integrity in the medium at the end of 21 days. At the 21st day of incubation, extract-loaded scaffolds degraded much faster up to 39% of its total weight compared to 34% for control unloaded scaffolds. This may arise from CQ dissolution to the degradation media that disintegrates the scaffold structure. Similarly, Soumya et al.<sup>36</sup> determined the degradation of CQ extract-loaded alginate/*O*-carboxymethyl CHI scaffolds and indicated that extract-loaded and CaCl<sub>2</sub> cross-linked scaffolds degraded up to 40% weight after 28 days of incubation.

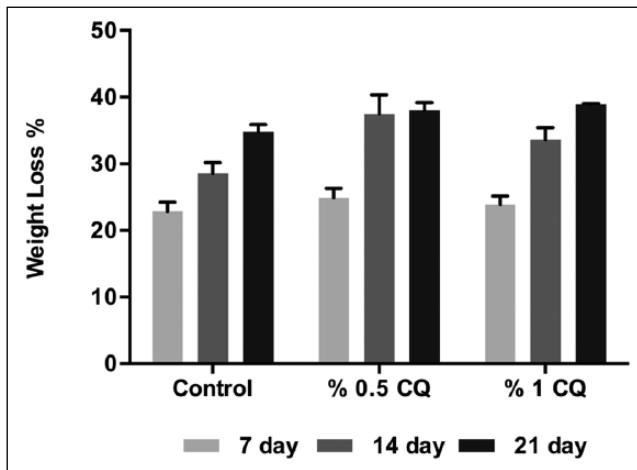


**Figure 5.** Weight loss % of CHI/Na-CMC, 0.5% and 1% CQ-loaded CHI/Na-CMC scaffolds during 21-day enzymatic degradation period with the presence of lysozyme.

*Cell attachment and proliferation on scaffolds.* Cell attachment on the scaffolds was investigated by DAPI staining. Fluorescence images depicted in Figure 7 showed that extract-loaded scaffolds provided a favorable surface for attachment and proliferation of SaOS-2 cells for 7 days of incubation. SaOS-2 cells attached and proliferated on pore surface of CQ-loaded CHI/Na-CMC scaffolds. CQ loading altered the pore surface serving an appropriate microenvironment for cell attachment.

### *In vitro studies*

*Cytotoxicity determination.* Cytotoxicity of scaffolds on SaOS-2 cells was evaluated by 24 h extraction of scaffolds according to ISO10993 standard. The extract has been tested on SaOS-2 cells with in vitro studies and found as non-toxic up to 100  $\mu\text{g/mL}$ .<sup>46,47</sup> In addition, in vivo toxicology studies of CQ extract have shown that CQ does not show any toxic effect.<sup>48</sup> In this study, scaffold extracts showed high cell viability % on SaOS-2 cell line. The cell viability % at 72 h was found as 70, 80, and 77.7 for the control group, 0.5% CQ and 1% CQ, respectively, by the interaction of scaffold extracts and SaOS-2 cells (Figure 6). Thus, both CHI/Na-CMC scaffold as a control group and CQ extract-loaded scaffolds did not show any cytotoxic effect on SaOS-2 cells.

The SaOS-2 proliferation on extract-loaded CHI/Na-CMC scaffolds for 28 days was examined with the fluorometric resazurin assay for 28 days. Significantly higher cell proliferation was obtained with 0.5% and 1% CQ extract-loaded scaffolds compared to control group for 7th, 14th, and 21st day of incubation (Figure 8). Increasing CQ extract concentration significantly affected SaOS-2 proliferation on early incubation periods (7 and 14 days) and decelerated for 21 and 28 days of incubation due to the overgrowth of cell population on scaffolds. Muthusami et al.<sup>46</sup> studied the effect of ethanolic extract of CQ itself on SaOS-2 cells and indicated that CQ treatment increased the proliferation of SaOS-2 cells. Similarly, Raghavan et al.<sup>49</sup> fabricated CQ extract-loaded poly(aryl ether ketone) (PAEK) scaffolds with soaking the scaffold in CQ extract solution and observed that incorporation of CQ extract increased SaOS-2 proliferation compared to control group.

*Alkaline phosphatase activity.* Alkaline phosphatase (ALP) activity is an early indicator and important factor for determination of osteogenic differentiation and critically involved in mineralization

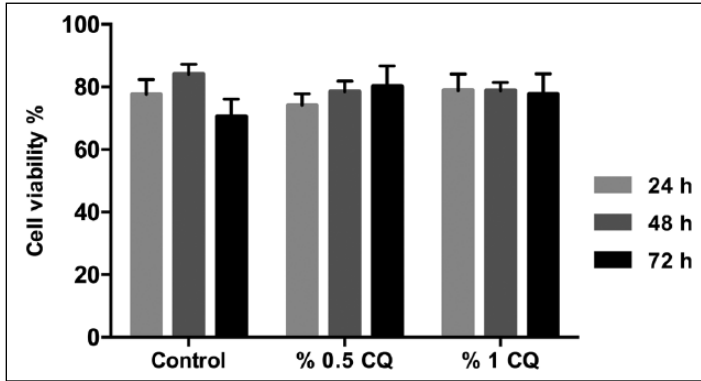


**Figure 6.** In vitro cytotoxicity of CHI/Na-CMC, 0.5% and 1% CQ-loaded CHI/Na-CMC scaffolds on SaOS-2 cell line for 24-, 48-, and 72-h incubation periods.

of osteoblasts. In this study, ALP activity was determined without osteogenic supplements in order to investigate the osteogenic effect of CQ extract on SaOS-2 cells. Figure 9 shows the ALP activity of SaOS-2 cells on scaffolds. Results showed that higher ALP activity was obtained on CQ-loaded CHI/Na-CMC scaffolds with increasing CQ concentration. A significant increase in ALP activity was obtained for 0.5% and 1% CQ concentrations compared to control group ( $p \leq 0.05$ ). The ALP activity of control group decreased at the early incubation periods because of the absence of an osteogenic medium. On the contrary, CQ extract incorporation promoted the ALP activity of SaOS-2 cells at 7 and 14 days of incubation periods. Our in vitro results showed that CQ extract loading enhanced the osteogenic differentiation by increasing ALP activity of SaOS-2 cells. However, at 28th day, SaOS-2 cells showed similar ALP activity on CQ-loaded scaffolds when compared with the control group. The decrease in ALP activity at 21 and 28 days may probably be due to high-level ALP expression induced during early osteoblast differentiation. The effect of pure CQ extract on ALP activity was investigated by Parisuthiman et al.,<sup>47</sup> and they indicated that the treatment of murine osteoblastic cells (MC) with CQ extract significantly increased ALP activity a dose-dependent manner. In the literature, the effect of CQ loading on different scaffolds were investigated and the positive effect of CQ extract on ALP activity was observed.<sup>35,36,49</sup>

**In vitro mineralization with von Kossa and Alizarin red staining.** In vitro mineralization results showed that CQ extract with high calcium and phosphate content induced the biomineralization of SaOS-2 cells on scaffolds. Stereomicroscopy images (Figure 10) show the calcium and phosphate deposition on scaffolds treated with von Kossa staining and alizarin red S staining. The images indicated that homogeneous distribution of mineral deposition was observed on CQ incorporated scaffolds compared to nonuniform mineral deposition on the control group. Similarly, the effect of CQ extract on mineralized matrix formation was investigated by observation of mineralized nodules and results indicated that mineralized nodules were dispersed on control cells, whereas they were extensively observed with CQ extract treatment.<sup>47</sup>

Microscopy images showed a high intensity of calcium and phosphate mineral depositions on CQ extract-loaded scaffolds which supported the ALP activity results observed for the 14th day since ALP is involved in an initiation of mineralization process during bone tissue formation by rendering extracellular matrices suitable for mineral deposition.<sup>50</sup> The quantitative results were supported with the elemental analysis on scaffold by XRF at 7th and 14th days of incubation. According to XRF results, similar calcium deposition was observed on control (3.34%) and 1% CQ-loaded

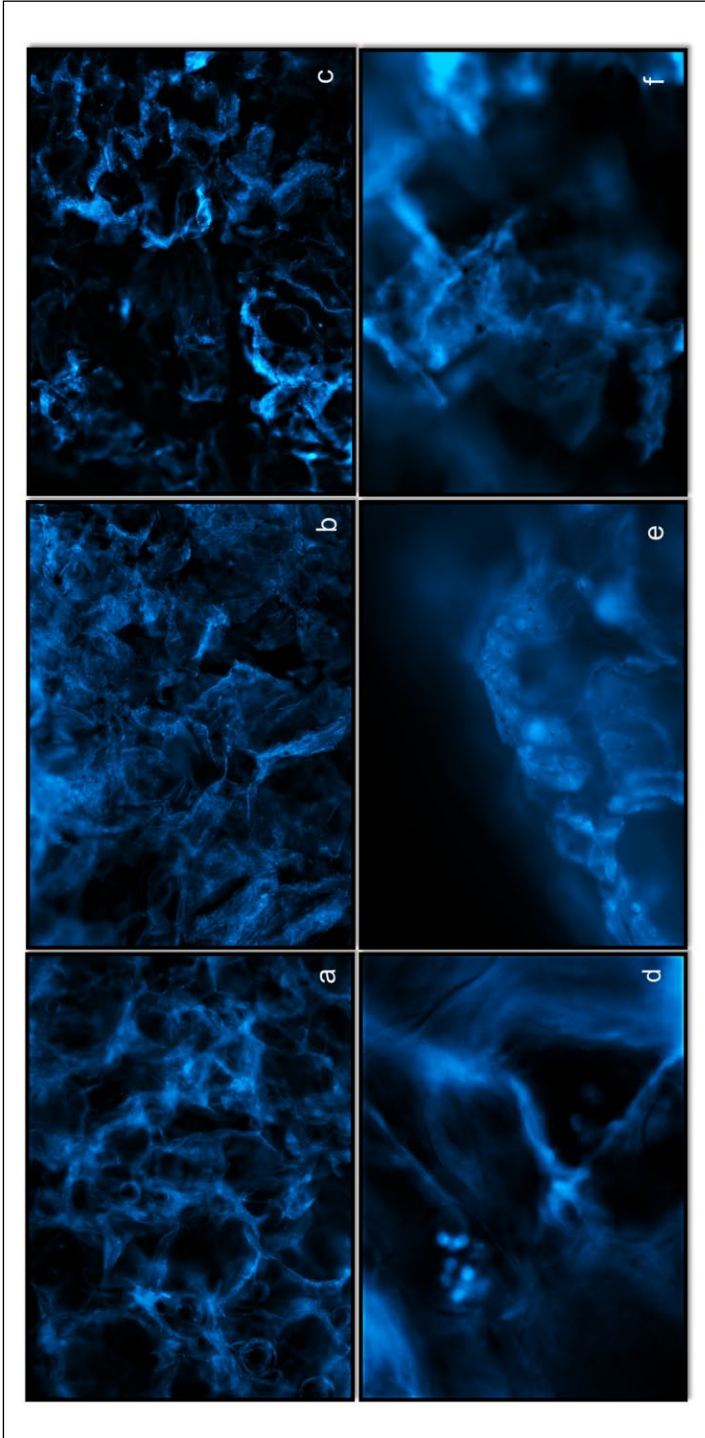


**Figure 7.** Fluorescence microscopy images of SaOS-2 cells cultured on (a, d) CHI/Na-CMC, (b, e) 0.5% CQ, and (c, f) 1% CQ-loaded CHI/Na-CMC scaffolds for 7 days.

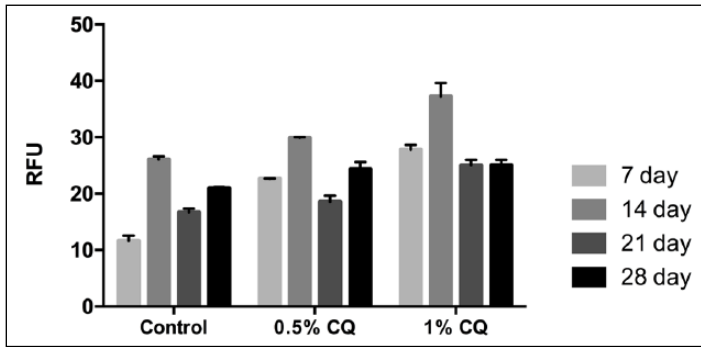


**Figure 8.** SaOS-2 proliferation on CHI/Na-CMC, 0.5% and 1% CQ-loaded CHI/Na-CMC scaffolds.

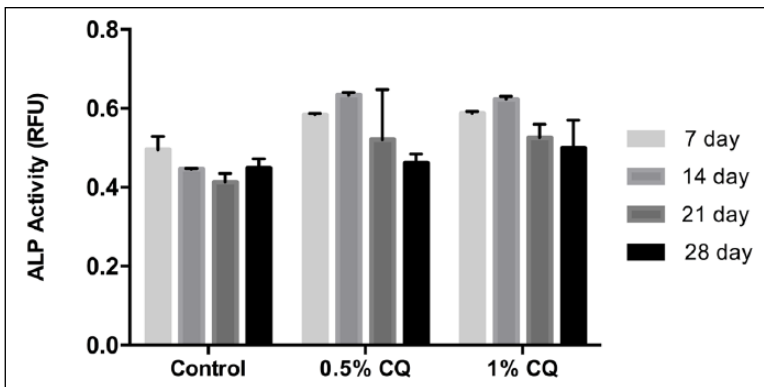


**Figure 9.** ALP activity of SaOS-2 cells cultured on CHI/Na-CMC, 0.5% and 1% CQ-loaded CHI/Na-CMC scaffolds.

scaffolds (3.37%) at 7th day of incubation. However, calcium deposition significantly increased on 1% CQ-loaded scaffolds (5.20%) at 14th day of incubation when compared to control group (4.18%). In addition, SEM analysis was performed to observe the mineralization on scaffolds at 14th day of incubation (Figure 11). As expected, biomineralization could not be observed on control group significantly in the absence of osteogenic supplement. Cell biomineralization was observed on CQ incorporated scaffolds even incubated in medium without osteogenic supplements.

## Conclusion

In this study, CQ ethanolic extract-loaded CHI/Na-CMC microporous scaffolds with the osteoinductive property have been developed for bone tissue engineering. CHI and Na-CMC blend was prepared to form a polyelectrolyte complex which enhanced the mechanical and physical properties of both CHI and Na-CMC biopolymers. Porous scaffolds were obtained with interconnected architecture. SEM images showed that CQ-loaded scaffolds were fabricated with appropriate pore size range for bone tissue formation. CQ extract loading to CHI/Na-CMC scaffolds significantly enhanced the mechanical strength for both wet and dry conditions. Besides, CQ extract, known as a remarkable traditional phytochemical for bone healing treatments due to its osteoinductive effect.

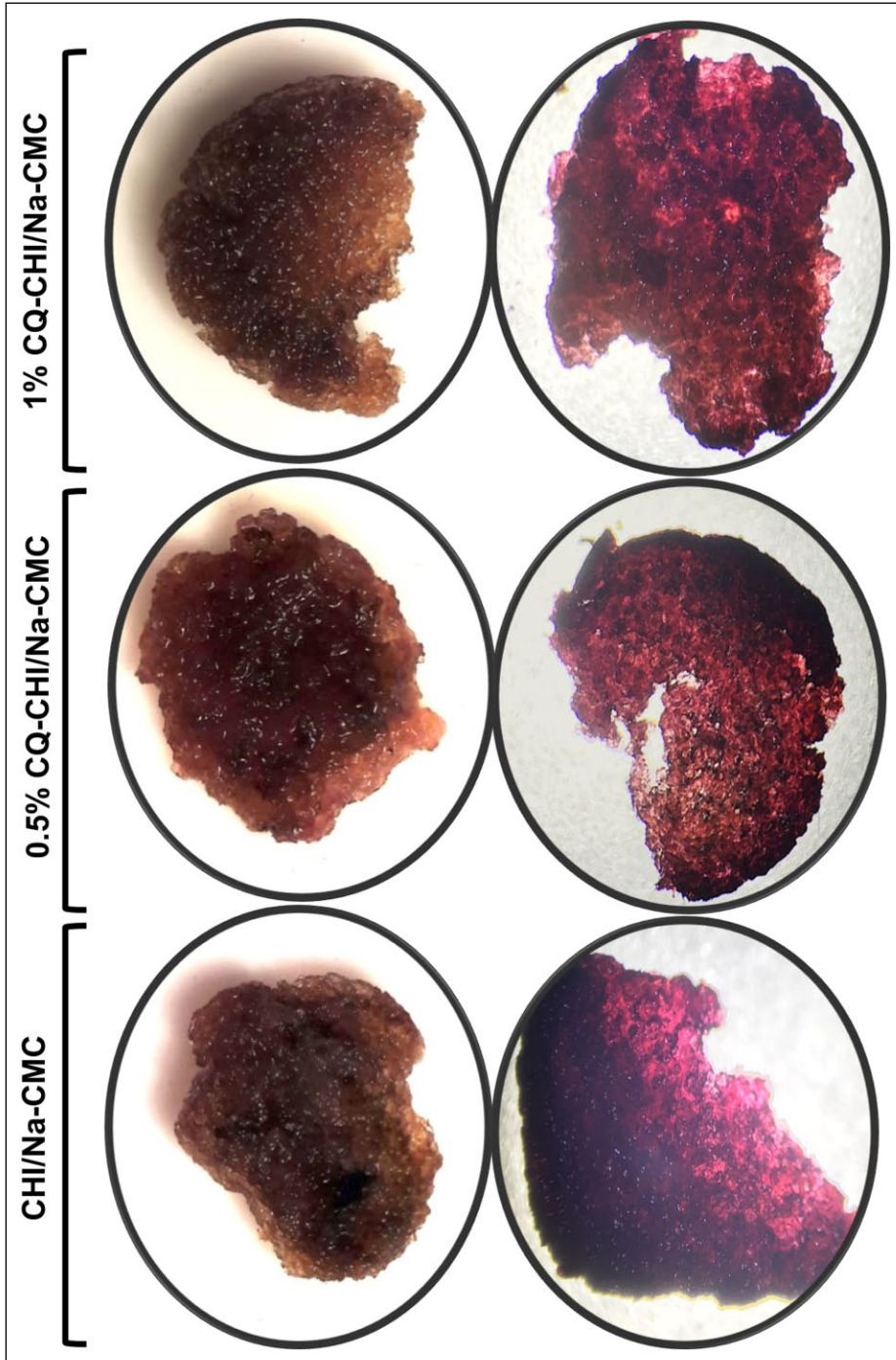


**Figure 10.** Stereomicroscopy images of von Kossa and Alizarin red staining on CHI/Na-CMC, 0.5% and 1% CQ-loaded CHI/Na-CMC scaffolds at 14th day.



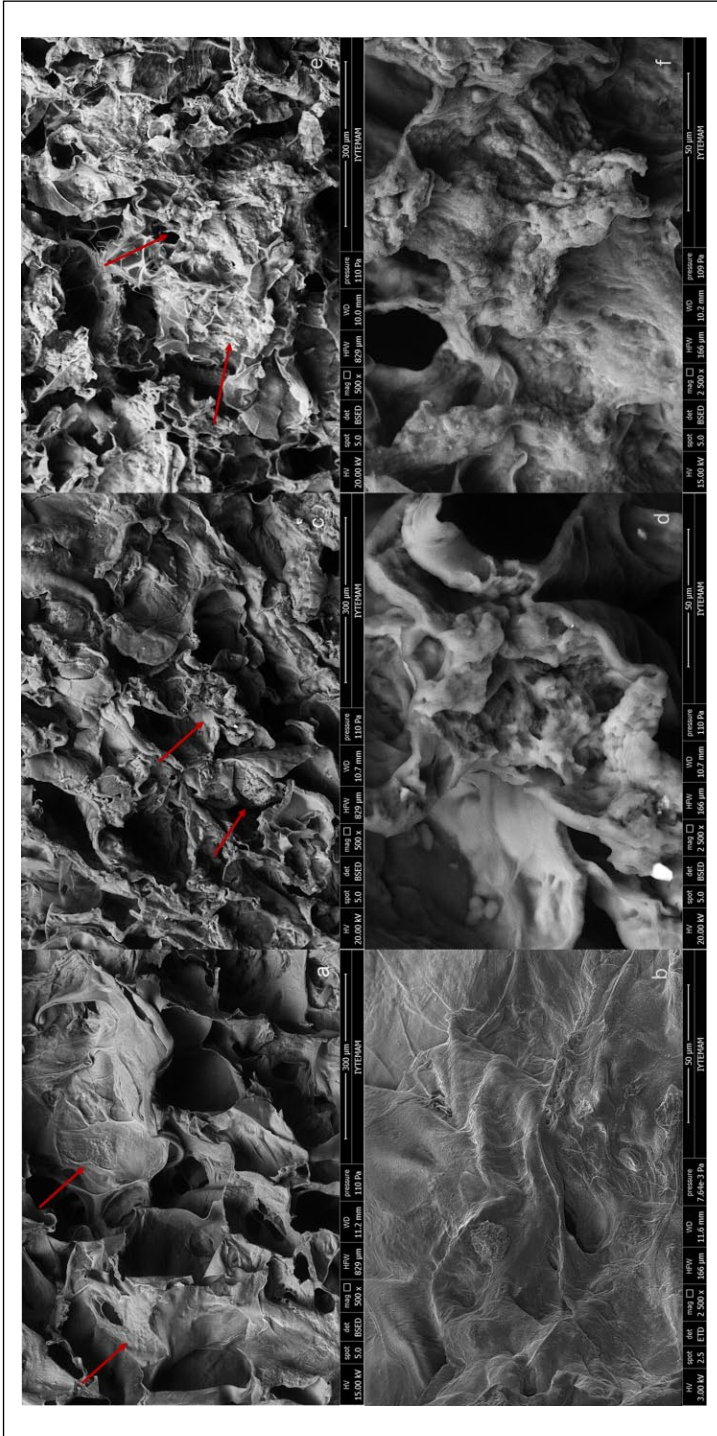


**Figure 11.** Scanning electron micrographs of biominaleralization on (a, b) CHI/Na-CMC, (c, d) 0.5% CQ, and (e, f) 1% CQ extract-loaded CHI/Na-CMC scaffolds, respectively.

Thus, it was incorporated into this polymer structure to induce the osteogenic activity. CQ-loaded scaffolds provided good mechanical and structural properties. The osteogenic effect of CQ extract was observed as early ALP activity and enhanced biomineralization on scaffolds. In conclusion, this study revealed that the bioactive CQ/CHI/Na-CMC scaffold is found to be a promising biomaterial for bone tissue engineering applications. In the future perspective of this work, some studies may still be needed to investigate the release profile of the extract and obtain a sustained release profile. Determination of active constituents responsible for osteogenic activities must be identified to reveal the bone healing mechanism.

### Acknowledgements

The authors thank Assistant Professor Dr Meltem Alper from Aksaray University for supplying SaOS-2 cell line. The authors are grateful to Izmir Institute of Technology Biotechnology and Bioengineering Research and Application Center (IZTECH BIOMER) for fluorescence microscopy analysis, Environmental Research Center of IZTECH for GC-MS analysis, and Center for Materials Research (IZTECH CMR) for SEM, stereomicroscopy imaging, and XRF analysis.

### Declaration of conflicting interests

The author(s) declared no potential conflicts of interest with respect to the research, authorship, and/or publication of this article.

### Funding

The author(s) received no financial support for the research, authorship, and/or publication of this article.

### References

1. Pillai CKS, Paul W and Sharma CP. Chitin and chitosan polymers: chemistry, solubility and fiber formation. *Prog Polym Sci* 2009; 34: 641–678.
2. Saravanan S, Leena RS and Selvamurugan N. Chitosan based biocomposite scaffolds for bone tissue engineering. *Int J Biol Macromol* 2016; 93: 1354–1365.
3. Seol YJ, Lee JY, Park YJ, et al. Chitosan sponges as tissue engineering scaffolds for bone formation. *Biotechnol Lett* 2004; 26: 1037–1041.
4. Senel S and McClure SJ. Potential applications of chitosan in veterinary medicine. *Adv Drug Deliv Rev* 2004; 56: 1467–1480.
5. Di Martino A, Sittinger M and Risbud MV. Chitosan: a versatile biopolymer for orthopaedic tissue-engineering. *Biomaterials* 2005; 26: 5983–5990.
6. Wang W and Wang A. Nanocomposite of carboxymethyl cellulose and attapulgite as a novel pH-sensitive superabsorbent: synthesis, characterization and properties. *Carbohydr Polym* 2010; 82: 83–91.
7. Xiao HJ, Hou CL, Guan SB, et al. Preparation and evaluation of chitosan-carboxymethyl cellulose membrane for prevention of postoperative intestinal adhesion: an experimental study. *Acad J Sec Mil Med Univ* 2006; 27: 755–759.
8. Qiu XL and Li GM. Preparation of low molecular weight heparin-chitosan-sodium carboxymethyl cellulose microcapsules and its drug-release performances. *Chinese J Pharm* 2005; 36: 690–693.
9. Tiitu M, Laine J, Serimaa R, et al. Ionically self-assembled carboxymethyl cellulose/surfactant complexes for antistatic paper coatings. *J Colloid Interf Sci* 2006; 301: 92–97.
10. Liuyun J, Yubao L and Chengdong X. Preparation and biological properties of a novel composite scaffold of nano-hydroxyapatite/chitosan/carboxymethyl cellulose for bone tissue engineering. *J Biomed Sci* 2009; 16: 65.
11. Sivarajan VV and Balachandran I. Ayurvedic drugs and their plant sources. 1st ed. New Delhi, India: Oxford & IBH Publishing, 1994, p. 570.
12. Kumar TS and Jegadeesan M. Physico-chemical profile of *Cissus quadrangularis* L. Var-i in different soils. *Anc Sci Life* 2006; 26: 50–58.
13. Chidambara Murthy KN, Vanitha A, Mahadeva Swamy M, et al. Antioxidant and antimicrobial



- activity of *Cissus quadrangularis* L. *J Med Food* 2003; 6: 99–105.
14. Onyechi UA, Judd PA and Ellis PR. African plant foods rich in non-starch polysaccharides reduce postprandial blood glucose and insulin concentrations in healthy human subjects. *Br J Nutr* 1998; 80: 419–428.
  15. Jainu M and Devi CS. In vitro and In vivo evaluation of free-radical scavenging potential of *Cissus quadrangularis*. *Pharm Biol* 2005; 43: 773–779.
  16. Jainu M and Devi CS. Gastroprotective action of *Cissus quadrangularis* extract against NSAID induced gastric ulcer: role of proinflammatory cytokines and oxidative damage. *Chem Biol Interact* 2006; 161: 262–270.
  17. Panthong A, Norkaew P, Kanjanapothi D, et al. Anti-inflammatory, analgesic and antipyretic activities of the extract of gamboge from *Garcinia hanburyi* Hook f. *J Ethnopharmacol* 2007; 111: 335–340.
  18. Stohs SJ and Ray SD. A review and evaluation of the efficacy and safety of *Cissus quadrangularis* extracts. *Phytother Res* 2013; 27: 1107–1114.
  19. Ghouse MS and Baig MS. Bone healing activity of *Cissus quadrangularis* Linn. *Int J Pharmacogn* 2015; 2: 527–531.
  20. Prabhavathi RM, Prasad MP and Jayaramu M. In-vitro antioxidant studies of *Cissus quadrangularis* (L) extracts. *Eur J Exp Bio* 2016; 6: 1–6.
  21. Sanyal A, Ahmad A and Sastry M. Calcite growth in *Cissus quadrangularis* plant extract, a traditional Indian bone-healing aid. *Curr Sci* 2005; 89: 1742–1745.
  22. Jakikasem S, Limsiriwong P, Kajsongkarm T, et al. Phytochemical study of *Cissus quadrangularis*. *Thai J Pharm Sci* 2000; 24: 5.
  23. Raghavan RN, Somanathan N and Sastry TP. Evaluation of phytochemical-incorporated porous polymeric sponges for bone tissue engineering: a novel perspective. *Proc Inst Mech Eng H* 2013; 227: 859–865.
  24. Shah UM, Patel SM, Patel PH, et al. Development and validation of a simple isocratic HPLC method for simultaneous estimation of phytosterols in *Cissus quadrangularis*. *Indian J Pharm Sci* 2010; 72: 753–758.
  25. Pathomwachaiwat T, Ochareon P, Soonthornchareonnon N, et al. Alkaline phosphatase activity-guided isolation of active compounds and new dammarane-type triterpenes from *Cissus quadrangularis* hexane extract. *J Etnopharmacol* 2015; 160: 52–60.
  26. Muthusami S, Ramachandran I, Krishnamoorthy S, et al. *Cissus quadrangularis* augments IGF system components in human osteoblast like SaOS-2 cells. *Growth Horm IGF Res* 2011; 21: 343–348.
  27. Udupa KN, Prasad G and Sen SP. The effect of phytogetic anabolic steroid in the acceleration of fracture repair. *Life Sci* 1995; 4: 317–327.
  28. Prasad GC and Udupa KN. Pathways and site of action of a phytogetic steroid from *Cissus quadrangularis*. *J Res Indian Med* 1972; 7: 29–34.
  29. Potu BK, Bhat KM, Rao MS, et al. Petroleum ether extract of *Cissus quadrangularis* (Linn.) enhances bone marrow mesenchymal stem cell proliferation and facilitates osteoblastogenesis. *Clinics* 2009; 64: 993–998.
  30. Mishra G, Srivastava S and Nagori BP. Pharmacological and therapeutic activity of *Cissus quadrangularis*: an overview. *Int J Pharmtech Res* 2010; 2: 1298–1310.
  31. Deka DK, Lahon LC, Saikia J, et al. Effect of *Cissus quadrangularis* in accelerating healing process of experimentally fractured radius-ulna of dog: a preliminary study. *Indian J Pharmacol* 1994; 26: 44–45.
  32. Shirwaikar A, Khan S and Malini S. Antiosteoporotic effect of ethanol extract of *Cissus quadrangularis* Linn. on ovariectomized rat. *J Ethnopharmacol* 2003; 89: 245–250.
  33. Banu J, Varela E, Bahadur AN, et al. Inhibition of bone loss by *Cissus quadrangularis* in mice: a preliminary report. *J Osteoporos*. Epub ahead of print 21 June 2012. DOI: 10.1155/2012/101206.
  34. Jain A, Dixit J and Prakash D. Modulatory effects of *Cissus quadrangularis* on periodontal regeneration by bovine-derived hydroxyapatite in intrabony defects: exploratory clinical trial. *J Int Acad Periodontol* 2008; 10: 59–65.
  35. Suganya S, Venugopal J, Ramakrishna S, et al. Herbally derived polymeric nanofibrous scaffolds for bone tissue regeneration. *J Appl Polym Sci*. Epub ahead of print 5 February 2014. DOI: 10.1002/app.39835.
  36. Soumya S, Sajesh KM, Jayakumar R, et al. Development of a phytochemical scaffold for bone tissue engineering using *Cissus quadrangularis* extract. *Carbohydr Polym* 2012; 87: 1787–1795.
  37. Berridge MV, Tan AS, McCoy KD, et al. The biochemical and cellular basis of cell proliferation

- assays that use tetrazolium salts. *Biochemica* 1996; 4: 14–19.
38. Meloan SN and Puchtler H. Chemical mechanisms of staining methods: von Kossa's technique: what von Kossa really wrote and a modified reaction for selective demonstration of inorganic phosphates. *J Histotechnol* 1985; 8: 11–13.
  39. Bonewald LF, Harris SE, Rosser J, et al. von Kossa staining alone is not sufficient to confirm that mineralization in vitro represents bone formation. *Calcif Tissue Int* 2003; 72: 537–547.
  40. Cheung HY, Lau KT, Lu TP, et al. A critical review on polymer-based bio-engineered materials for scaffold development. *Compos Part B: Eng* 2007; 38: 291–300.
  41. Rosca C, Popa MI, Lisa G, et al. Interaction of chitosan with natural or synthetic anionic polyelectrolytes. 1. the chitosan-carboxymethylcellulose complex. *Carbohydr Polym* 2005; 62: 35–41.
  42. Song JY, Jang HK and Kim BS. Biological synthesis of gold nanoparticles using *Magnolia kobus* and *Diospyros kaki* leaf extracts. *Process Biochem* 2009; 44: 1133–1138.
  43. Eswaran R, Anandan A, Doss A, et al. Analysis of chemical composition of *Cissus quadrangularis* Linn by GC-MS. *Asian J Pharm Clin Res* 2012; 2: 139–140.
  44. Thakur A, Jain V, Hingorani L, et al. Phytochemical studies on *Cissus quadrangularis* Linn. *Pharmacogn Res* 2009; 1: 213–215.
  45. Noguchi TS, Fujioka TS, Choe S, et al. Biosynthetic pathways of brassinolide in Arabidopsis. *Plant Physiol* 2000; 124: 201–210.
  46. Muthusami S, Senthilkumar K, Vignesh C, et al. Effects of *Cissus quadrangularis* on the proliferation, differentiation and matrix mineralization of human osteoblast like SaOS-2 cells. *J Cell Biochem* 2011; 112: 1035–1045.
  47. Parisuthiman D, Singhatanadgit W, Dechatiwongse T, et al. *Cissus quadrangularis* extract enhances biomineralization through up-regulation of MAPK-dependent alkaline phosphatase activity in osteoblasts. *In Vitro Cell Dev Biol Anim* 2009; 45: 194–200.
  48. Attawish A, Chavalittumrong P, Chivapat S, et al. Subchronic toxicity of *Cissus quadrangularis* Linn. *Songklanakarinn J Sci Technol* 2002; 24: 39–51.
  49. Raghavan N, Dare BJ, Somanathan N, et al. Evaluation of phytochemical-incorporated porous polymeric sponges for bone tissue engineering: a novel perspective. *Trends Biomater Artif Organs* 2015; 29: 188–192.
  50. Lian JB, Stein GS, Canalis E, et al. Bone formation: osteoblast lineage cells, growth factors, matrix proteins and the mineralization process. In: Favus MJ (ed.) *Primer on the Metabolic Bone Diseases and Disorders of Mineral Metabolism*. 4th ed. Philadelphia, PA: Lippincott Williams & Wilkins, 1999, pp. 14–29.